Effective shear stress of graded sediments

D. Buscombe[1] and D. C. Conley[1]

Received 17 December 2010; revised 20 March 2012; accepted 20 March 2012; published 3 May 2012.

[1] A meta-analysis of fractional mobilization data from 14 sets of experiments, totaling 103 different mixed sand and gravel beds and flow conditions, has been carried out in order to identify an expression for effective shear stress, here defined as the component of bed shear stress that is directly involved in transporting each grain size fraction in graded sediment. In doing so we test the assumption that excess stress should be defined solely in terms of a critical stress rather than effective stress, which exhibits sensitivity to the flow stage. In contrast to the approach which evaluates the size-distribution effects on motion threshold by comparing inferred transport rates, an alternative approach is utilized which is based on the skill of reproducing the measured, mobilized particle size distribution. A simple equation is developed for mobilization of sediment mixtures, based on a well-established transport law, and employing a classical "hiding function" approach to the problem of mitigating the bias toward mobilizing fine material in the mixture. We use inverse methods to find the optimal form of the hiding function which provides the best fit with the data. We find that the hiding function is indeed sensitive to the flow and bed composition. On this basis, a simple deterministic equation is proposed for fraction-specific effective stress, which outperforms the next best existing formula based on critical stress by 34% on aggregate.

Citation: Buscombe, D., and D. C. Conley (2012), Effective shear stress of graded sediments, *Water Resour. Res.*, *48*, W05506, doi:10.1029/2010WR010341.

1. Introduction

[2] It is generally accepted that volumetric sediment transport rate per unit width, q, is related to bed shear stress, τ, such that $q = \mathbf{f}(\tau^n)$. If bed shear stress is nondimensionalized as,

$$\theta = \frac{u_*^2}{RgD} \tag{1}$$

(known as the Shields parameter after *Shields* [1936]), in which $u_* = \sqrt{\tau/\rho}$ is shear velocity, $R = (\rho_s - \rho)/\rho$ is specific sediment density, and ρ, ρ_s are the densities of fluid and sediment, respectively, g is gravitational acceleration, and D is grain diameter, nondimensionalized volumetric sediment transport rate (or sediment flux) is expressed as $q^* = \mathbf{f}(\theta^{n/2})$, where

$$q^* = \frac{q}{\sqrt{RgD^3}}. \tag{2}$$

[3] To highest order, a large proportion of such models can be represented as $q^* = \mathbf{f}(\theta^{3/2})$ [e.g., *Meyer-Peter and Müller*, 1948; *Einstein*, 1950; *Ashida and Michiue*, 1972; *Bagnold*, 1973; *Fernandez-Luque and Van Beek*, 1976; *Kachel and Sternberg*, 1971; *Parker and Klingeman*, 1982; *Wiberg and Smith*, 1989; *Wong and Parker*, 2006] but alternatives exist, and are suggested predominantly for oscillatory flows, such as $q^* = \mathbf{f}(\theta^{4/2})$ [e.g., *Sleath*, 1978], $q^* = \mathbf{f}(\theta^{5/2})$ [e.g., *Hanes and Bowen*, 1985], and $q^* = \mathbf{f}(\theta^{6/2})$ [e.g., *Madsen and Grant*, 1976].

[4] *Shields* [1936] introduced the concept of a critical normalized shear stress, θ_c, necessary to initiate sediment motion (the "mobility" of the sediment). The existence of such a threshold implies $q = 0$ when $\theta < \theta_c$, where θ_c represents a critical value of the Shields parameter, which is the value of the Shields parameter at incipient motion. The critical Shields parameter is commonly given as a function of grain Reynolds number:

$$Re_g = \frac{u_* D}{\nu}, \tag{3}$$

where ν is the kinematic viscosity of the fluid. A commonly used sediment transport model, which was one of the first to attempt to account for the implications of threshold conditions, is that of *Meyer-Peter and Müller* [1948] given by:

$$q^* = 8(\theta - 0.047)^{3/2}. \tag{4}$$

[5] The fact that their "threshold" is a constant is unsurprising given that for the majority of their experiments $Re_g > 10^2$, for which θ_c is a constant ≈ 0.047. It has since become common practice in much of deterministic sediment transport modeling to include a critical Shields parameter to provide the mathematical consistency for the

[1]School of Marine Science and Engineering, University of Plymouth, Plymouth, UK.

0043-1397/12/2010WR010341

fact that transport does not occur at stress values below this critical value, and to acknowledge that some level of stress applied by the fluid on the bed is expended on processes other than the transport of sediment. Conceptually, this is represented symbolically as,

$$q^* = \alpha(\theta - \theta_c)^{3/2}, \tag{5}$$

where it is clear that the $n = 3$ convention has been adopted as it will be for most of the remainder of this work, and where α is a parameter, the functional form of which is dependent on the sediment transport model. The quantity in brackets is referred to as the excess stress and represents the amount of the bed stress, which may be assumed to be transporting the sediment load. The quantity of bed stress not transporting sediment in (5) is given by the critical stress (θ_c), an analytical expression given by *Soulsby* [1997]:

$$\theta_c = \frac{0.3}{1 + 1.2D^*} + 0.055[1 - \exp(-0.02D^*)], \tag{6}$$

where dimensionless grain size, D^* is given as,

$$D^* = \left[\frac{g(\rho_s/\rho - 1)}{\nu^2}\right]^{1/3} D. \tag{7}$$

[6] The relatively unchallenged assumption in expressions such as (5) is that the quantity of bed stress not expended in transport is constant and independent of the flow or transport stage. Examination of this assumption is one of the major goals of this work.

[7] Approaches to the determination of motion threshold for a sediment fraction in a mixture based on explicit force-moment balance [*Allen*, 1985], or in terms of grain-resisting stress [*Wiberg and Smith*, 1987], or the probabilistic description of relative exposure of grains [*Wu et al.*, 2000], which result in models that produce a shape similar to the Shields curve, and are operationally more difficult to implement. That is because they require specification of quantities, such as lift/drag forces and particle packing angles [*Wiberg and Smith*, 1987], which vary on such small spatial and temporal scales as to make their implementation impractical.

2. Critical Stress of Graded Sediment

[8] Significant scatter in the Shields relation exists when using data sets from a wide variety of flows and sediments [*Wilcock*, 1988; *Buffington and Montgomery*, 1997]. In consequence, considerable attention has been given to how the presence of a distribution of grain sizes affects sediment mobility. Numerous experiments have shown that in a sediment bed containing a mixture of sizes, the response exhibited by any particular grain size fraction at a given shear stress, is different from what would be expected if the bed were uniformly composed of that fraction [*Einstein*, 1950; *Egiazaroff*, 1965; *Day*, 1980; *Wilcock and Southard*, 1988; *Wilcock and McArdell*, 1993]. A simplistic, and perhaps obvious generalization of equation (5) to be applicable in the presence of a distribution of grain sizes D_i is,

$$q_i^* = \alpha[(\theta_i - \theta_{c_i})^{3/2} P_i], \tag{8}$$

where P_i is the relative proportion of the i-th fraction in the bed $\left(\sum P_i = 1\right)$ and q_i^* represents the total transport rate of the i-th sediment class. While some transport formulas use these assumptions [e.g., *Yang and Wan*, 1991], most data has shown that equation (8) typically overpredicts the fine-grain contribution to the transport size distribution when the standard deviation of the bed material is sufficiently large [*Wilcock*, 1988; *Buffington and Montgomery*, 1997]. Thus, it has become clear that graded sediment cannot be considered as a generalization of insights obtained from the simpler uniform case, and further that it is not enough to generalize formulations for uniform sediment in a simple and direct way to account for the existence of a variety of grain sizes [*Proffitt and Sutherland*, 1983; *Komar*, 1987; *Bridge and Bennett*, 1992; *Kleinhans and van Rijn*, 2002; *Wilcock and Crowe*, 2003]. The observed overprediction of fine-grain transport and the underprediction of the coarser component implies that sediment is more equally mobile than that predicted by calculating θ_c for each size class (θ_{c_i}). To account for this, many currently applied approaches apply a small adjustment to equation (8) so that the bed stress terms individually normalized for all grain classes θ_i are replaced with a common stress value expressed in terms of the Shields parameter θ_g for a representative grain size D_g such that:

$$q_i^* = \alpha[(\theta_g - \theta_{c_i})^{3/2} P_i]. \tag{9}$$

[9] Standard statistical grain sizes ($\overline{D}$, D_{50}, D_{65}, etc.) are generally utilized for the nominal grain size D_g. Next, a long known approximation first observed by *Einstein* [1950] is used, which states that the ratio of critical Shields parameters for two different grain sizes can be approximated as the inverse ratio of diameters alone. Adapting this observation for inclusion in equation (9), it can be stated:

$$\theta'_{c_i} = \theta_{c_g}\left(\frac{D_i}{D_g}\right)^{-1}. \tag{10}$$

[10] Defining all θ'_{c_i} as a simple modification of a single θ_{c_g} is more easily tractable, both theoretically and practically. Finally, correcting the misprediction of the mobile grain-size distribution commonly involves the introduction of a weighting function in relation to the apparent critical stress, which generally serves to mitigate the bias toward fine material in transport relations. These so-called "hiding" or "hiding-exposure" corrections to mobility are supposed to quantify the degree to which differences in exposure and friction angles tend to offset differences in particle weight [*Buffington et al.*, 1992]. Various forms have been suggested [*Einstein*, 1950; *Egiazaroff*, 1965; *Ackers and White*, 1973], however, all forms to date can be expressed in power form using an exponent to account for the effects related to the presence of a distribution of grains [*Wilcock*, 1988; *Bridge and Bennett*, 1992]. Defining θ'_{c_i} in terms of the exponent b and making use of equation (10) it can be written:

$$\theta'_{c_i} = \theta_{c_g}\left(\frac{D_i}{D_g}\right)^{b-1}. \tag{11}$$

[11] It has been suggested that theoretical approaches such as *Wiberg and Smith* [1987] can be expressed in a form similar to (11), partly because pivot angle decreases with decreasing D_i/D_g [*Bridge and Bennett*, 1992]. However, the literature is contradictory as to whether b should be a scalar which applies to all D_i (i.e., b), or whether the exponent should be varied for each size class (i.e., b_i). The essential difference is that a single b means critical stress is a linear function of grain size [*Milhous*, 1973; *Carling*, 1983; *Hammond et al.*, 1984], and b_i implies that a nonlinear relationship exists [*Day*, 1980; *Wilcock and Crowe*, 2003]. Formulas to date suggest $b_i = \mathbf{f}(D_g)$ [*Egiazaroff*, 1965; *Ashida and Michiue*, 1972], $b_i = \mathbf{f}(D_g, \sigma)$ [*Wilcock and Crowe*, 2003], or $b = \mathbf{f}(D_g, \sigma)$ [*Shvidchenko et al.*, 2001], where σ is related to the standard deviation of particle sizes (for example, sand content or sorting coefficient).

[12] When $b = 0$ there is no mitigation of selective fine mobilization and the apparent critical stress is identical to the critical stress for uniform sediments. If $0 < b < 1$, there is partial mitigation of fine mobilization which varies nonlinearly with the value of b. In other words, the hiding function reduces but does not eliminate the tendency for preferential mobilization of finer surface grains. The condition $b = 1$ represents the limit where all grains are equally mobile [e.g., *Parker and Klingeman*, 1982], and the highly unrealistic case of $b > 1$ represents conditions in which coarser grains are more readily entrainable than the fine grains (see reviews by *Komar* [1987], *Wilcock* [1988], and *Buffington and Montgomery* [1997]).

3. Effective Stress of Graded Sediment

[13] Adaptation of the results of section 2 into an equation for the transport of each grain size based on excess stress would result in a form of the type:

$$q_i^* = \alpha[(\theta_g - \theta'_{c_i})^{3/2} P_i]. \tag{12}$$

[14] This equation suffers, however, from the same unspoken assumption associated with equation (5), namely that the amount of stress which does not contribute to transporting sediment is independent of the flow conditions and identical to the critical stress.

[15] While this assumption has not traditionally received much attention, recent studies [*Zanke*, 2003; *Cheng*, 2004, 2006] suggest it may not be valid. We define the quantity *effective* shear stress, τ_e, as the stress applied by the flow on the bed which is expended on processes other than mobilization of sediment. The nature of turbulent excitation exerted on a sediment bed has been shown to significantly affect excess stress [*Sumer et al.*, 2003; *Cheng*, 2006]. The observation made by *Cheng* [2006] is that θ_c is a limiting case of θ_e, and that the equivalence or otherwise of these two quantities is flow dependent.

[16] These observations are supported by other experimental evidence. *Meyer-Peter and Müller* [1948], for example, observed that their "specific gravity" coefficient $A = 0.047$ (later taken to be θ_c in line with *Shields* [1936], as noted by (5)) at "the beginning of bed load transport" actually reduced to 0.03 "at absolute rest" and up to 0.05 under higher τ [*Wong and Parker*, 2006]. The dependence of b on just D_i/D_g even in critical stress observations is not entirely satisfactory considering both *Day* [1980] and *Ashworth and Ferguson* [1989] report differing optimal b for constant values D_i/D_{50} with differing flow conditions. Finally, a meta-analysis by *Nielsen* [1992] suggested that a better fit to available data would be obtained if α in equation (4) was a function of θ.

[17] The above suggests that the excess stress term in (12) becomes $(\theta_g - \theta_{e_i})$, and an excess stress formulation based on an effective stress which exhibits flow dependence may be more appropriate than one based on critical stress. Nonetheless, it is believed that the experience gained in accounting for the effects of grain-size distributions on critical stress is valuable and that the approach inherent in (11) can be applied to effective stress as follows:

$$\theta_{e_i} = \theta_{c_g}\left(\frac{D_i}{D_g}\right)^{b-1} \tag{13}$$

therefore,

$$q_i^* = \mathbf{f}(\theta_g - \theta_{e_i}) = \mathbf{f}\left[\theta_g - \theta_{c_g}\left(\frac{D_i}{D_g}\right)^{b-1} P_i\right]. \tag{14}$$

[18] In this contribution we use functional analysis and inverse methods in order to determine the form of b. As in the traditional treatment of critical stress for graded sediments, we shall look for a functional dependence of the effective stress related b on D_g and σ. However, in light of the preceding discussion, the possibility of effective stress dependence on flow parameters shall also be entertained by searching for evidence of a b dependence on u_*.

[19] A common approach in the determination of θ'_{c_i} (as defined by equation (11)) is the so-called "reference transport" method whereby the (per grain-size) reference stress θ_{ri} (also termed the similarity parameter) is defined as the value of θ at which a small, yet measurable, quantity of normalized transport rate is equal to a reference value [*Ashida and Michiue*, 1972; *Wilcock*, 1988]. Definitions of b are then based on matching modeled and measured q_i. Common models for normalized transport rate are the Einstein parameter:

$$q_i^* = \frac{q_i}{P_i \rho_s \sqrt{(\rho_s/\rho_f - 1) g D_i^3}} \tag{15}$$

and the parameter defined by *Parker et al.* [1982]:

$$W_i^* = \frac{(\rho_s/\rho_f - 1) g q_i}{P_i u_*^3}. \tag{16}$$

[20] The reference level used by *Shvidchenko et al.* [2001] in conjunction with equation (15) is the stress which produces transport rate $q_i^* = 10^{-4}$, and that used by *Wilcock and Crowe* [2003] in conjunction with equation (16) is the stress which produces transport rate $W_i^* = 0.002$. If transport observations do not capture the threshold condition (all observed normalized transport rates are greater than the reference value) then one must extrapolate from the observations back to the reference value. In doing so, an assumption is made regarding the nature of the variation of transport

with stress, usually that the transport is a very steep and the linear function of stress is near the threshold condition. This approach naturally introduces elements of uncertainty, not the least of which is the appropriate choice of models (equations (15) and (16)), which can result in up to a 30% difference in values of reference shear stress [*Shvidchenko et al.*, 2001].

[21] In addition, the use of a reference approach introduces another level of abstraction, namely that which relates to the correct transport model (i.e., α in equation (5)). This subject, independent of the subject of mixed grain sizes, is the topic of energetic discussion for which there are numerous well-established formulas (see reviews by, for example, *Buffington and Montgomery* [1997] and *van Rijn* [2007]). In addition, measurements of volumetric transport rate per size fraction are sensitive to (possibly cumulative) errors in both size class-based estimates of sediment load and velocity.

[22] The chosen framework (equation (13)) incorporates the often-used hypothesis that a single fractional transport function can be defined in terms of the excess stress (equation (9)) using similarity principles [*Ashida and Michiue*, 1972; *Wilcock*, 1988]. However, an attractive feature of the present approach is that it avoids the issues associated with the uncertainties in direct modeling of fractional transport rate. Thus, in order to determine b and, by extension, θ_{e_i}, it is argued that a more productive exercise is to focus on comparing measured integrated transport load per size fraction and inferred mobilized particle size distribution, P_{m_i}, rather than measured and modeled q_i. The predictive relationship identified for b will be evaluated on its ability to reproduce P_{m_i} from measured integrated transport load across the whole range of D_i. To do so, a mobility function is introduced which is a linear function of bed shear stress. Continuing with our substitution of θ_c with θ_e, the total (volumetric) sediment load per unit area of the bed, l, can be expressed as [*Bagnold*, 1956; *Sawamoto and Yamashita*, 1986]:

$$l = \int_0^h c(z)dz \propto (\theta_g - \theta_e), \tag{17}$$

where h and z are water depth and vertical coordinate, respectively. Under steady conditions a typical sediment velocity, u_s, can be introduced where [*Nielsen*, 1992; *Lajeunesse et al.*, 2010]:

$$q = u_s l. \tag{18}$$

[23] Recognizing that concentration (c), load (l), and transport (q) are all considered sums of their respective individual size classes $\left(\text{or } c = \sum_{i=1}^{I} c_i;\ l = \sum_{i=1}^{I} l_i;\ \text{and } q = \sum_{i=1}^{I} q_i\right)$, and assuming that the proportion of excess stress utilized to mobilize a sediment size class is equal to the proportion of the bottom sediments (P_i) it represents, using equation (13) with equation (17) it is recognized that:

$$l_i \propto \left[\theta_g - \theta_{c_g}\left(\frac{D_i}{D_g}\right)^{b-1}\right]P_i. \tag{19}$$

[24] Further, if the reasonable first-order assumption is made that the scalar quantity $u_s \propto \sqrt{\theta_g}$ [e.g., *Bagnold*, 1973; *Wiberg and Smith*, 1989; *Lajeunesse et al.*, 2010], it becomes clear that the only fashion in which equation (18) can be consistent with equation (14) is if:

$$q_i \propto u_s\left[\theta_g - \theta_{c_g}\left(\frac{D_i}{D_g}\right)^{b-1}\right]P_i. \tag{20}$$

[25] Notice that this is consistent with the common result $q^* = \mathbf{f}(\theta^{3/2})$. It is now possible to focus on determining θ_{e_i} by comparing predicted and measured sediment load distributions. If l is a linear function of excess shear stress (equation (17)), given $P = \sum_{i=1}^{I} P_i$ and $P_m = \sum_{i=1}^{I} P_{m_i}$ it may be stated:

$$\begin{aligned} P_{m_i} &= \frac{\int u_s(\theta_g - \theta_{e_i})P_i dt}{\int \sum u_s(\theta_g - \theta_{e_i})P_i dt}, \\ &= \frac{\left(\theta_g - \theta_{c_g}\left[\frac{D_i}{D_g}\right]^{b-1}\right)P_i}{\sum_{i=1}^{I}\left[\theta_g - \theta_{c_g}\left(\frac{D_i}{D_g}\right)^{b-1}P_i\right]}. \end{aligned} \tag{21}$$

[26] It is now clear that, given measurements of total transport for each of the grain size fractions, P_{m_i} can be determined by normalizing the transport for each class size with the total transport. Once P_{m_i} are known, given u_*, D_i, D_g, and P_i it is possible to use the right-hand side of equation (21) to solve for b.

4. Methods and Data

[27] The optimal b were determined using a nonlinear optimization scheme to minimize ψ, the root-mean-square (RMS) of residuals between the observed P_{m_i} and those estimated using the right-hand side of equation (21). For the optimization, b was constrained to the interval $[-2, 2]$, which is greater than the range of reported values for b in the literature. The test data set was limited to previously published data from controlled steady state field and sediment recirculating laboratory experiments which provided quantitative information on net transport for each class size.

[28] In order to apply equation (21) across as broad conditions as possible while avoiding issues related to cohesion, conditions were sought where the bed sediment particle size distribution (P_i) is sand or mixed sand and gravel, and where the flow conditions allow both partial and full mobilization of the same bed sediment. Using these criteria, a test data set consisting of 14 sets of experiments totaling 103 different bed and flow conditions was compiled. The experimental conditions are summarized in Table 1. In each, the data consisted of measured P_i and integrated load (both volume-by-weight) and stated as u_*. Figure 1 depicts the P_i (both unimodal and bimodal) for the 14 sets of experiments. The last column in Table 1 is the sediment bi-modality index of *Sambrook-Smith et al.* [1997] defined as,

$$B = |\phi_2 - \phi_1|\frac{P_2}{P_1}, \tag{22}$$

Table 1. Summary of Experimental Conditions for the Data Used in This Study[a]

Experiment	Flume	Published	θ_g	D_i/D_g	D_g (mm)	σ (mm)	Mean B
Series A	R	*Day* [1980]	0.71 → 0.96	0.02 → 3.49	2.5	2.48	3.36
Series B	R	*Day* [1980]	0.54 → 1.08	0.03 → 3.03	1.84	1.51	9.62
Series T	R	*Blom and Kleinhans* [1999]	0.42 → 0.61	0.055 → 4.97	2.8 → 3.5	3.55 → 3.95	5.49
SG10	R	*Kuhnle* [1993]	0.27 → 0.92	0.22 → 8.35	0.97	1.52	0.52
SG25	R	*Kuhnle* [1993]	0.59 → 1.11	0.12 → 4.79	1.7	2.14	1.24
SG45	R	*Kuhnle* [1993]	0.25 → 0.52	0.081 → 3.21	2.6	2.45	3.65
BMC	R	*Wilcock and McArdell* [1993]	0.12 → 0.46	0.017 → 9.12	5.1 → 6	7.97 → 13.42	6.34
J6	R	*Wilcock et al.* [2001]	0.25 → 0.27	0.0058 → 3.11	14.5 → 17.1	9.95 → 12	0
J14	R	*Wilcock et al.* [2001]	0.21 → 0.41	0.0062 → 3.19	14.2 → 16.2	11.2 → 11.9	0
J21	R	*Wilcock* et al. [2001]	0.20 → 0.47	0.02 → 6.15	7.3 → 9.16	10.3 → 11.96	3.55
J27	R	*Wilcock et al.* [2001]	0.15 → 0.54	0.03 → 7.35	6.1 → 7.6	10.3 → 11.9	4.44
Sun	R	*Sun and Donahue* [2000]	0.59 → 0.99	0.18 → 7.9	0.7 → 1.08	0.55 → 1.16	0
Tait	R	*Tait et al.* [1992]	0.74 → 1.00	0.03 → 2.05	3.1 → 3.4	1.48 → 1.57	0
Goodwin	Field	*Kuhnle* [1992]	0.22 → 0.37	0.0079 → 4.26	15.72	18.96	7.91

[a]R and field denote sediment-recirculating flume and field data, respectively. $B = 0$ is unimodal.

where subscripts 1 and 2 refer to the distribution modes in the fine and coarse grain sizes, respectively, and ϕ is the grain size in phi units defined by $\phi = -\log 2[D(mm)]$. The P_i for the BMC, J6, J14, J21, and J27 data sets were compiled using surface photographs [*Wilcock et al.*, 2001], and as such they are areal, frequency-by-number [*Kellerhals and Bray*, 1971]. Following *Wilcock and Crowe* [2003], the appropriate weighting function provided by *Diplas and Frip* [1992] was therefore applied to these P_i data using the weighting parameter recommended by *Kellerhals and Bray* [1971] for sand/gravel mixtures.

[29] The literature on hiding function approaches to the initial motion of mixtures uses both mean [*Ashida and Michiue*, 1972; *Parker*, 1990; *Pender and Li*, 1995] and median [*Egiazaroff*, 1965; *Proffitt and Sutherland*, 1983; *Wilcock and Crowe*, 2003] as the correct specification of D_g, with apparently little justification for the selection of one over the other. Here arithmetic mean grain size $\left(D_g = \sum_{i=1}^{I} D_i P_i\right)$ was chosen because, as a moment of the size density function, it is analytically more tractable, which is important in this case where a generalized form of the hiding function is sought. This is especially true if the sedimentologic (phi) transform is employed. While it is true the mean responds proportionately greater than the median to distribution skew, it is not in this case being used as

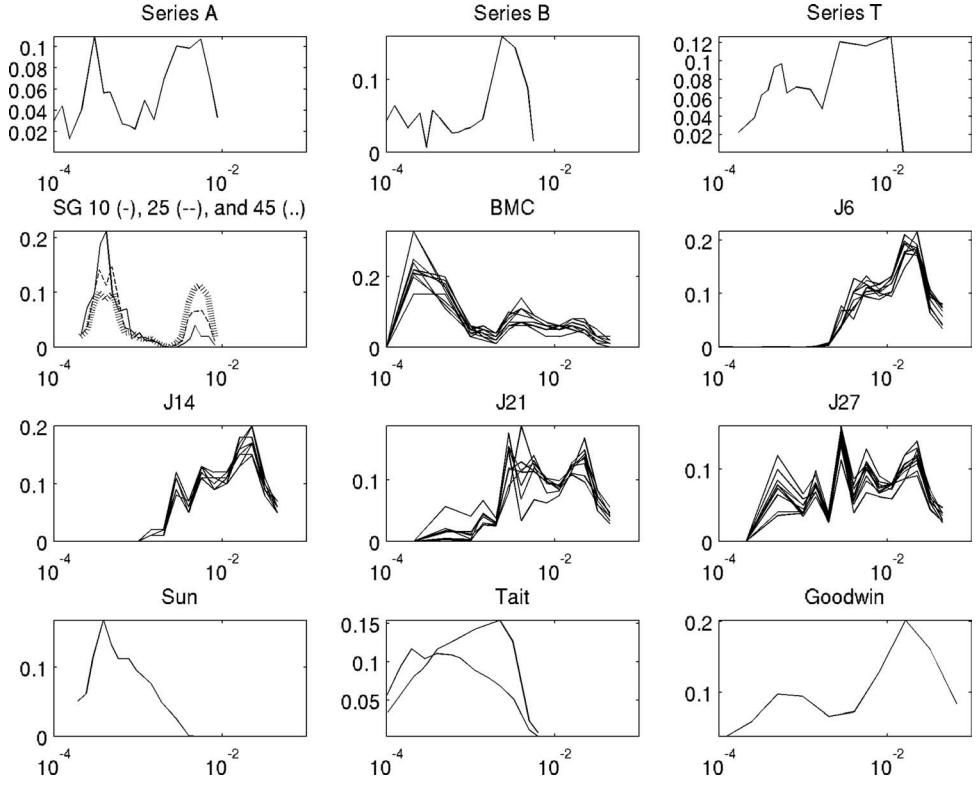

Figure 1. Bed sediment particle size distributions used in the experimental work.

a statistic of central tendency. For each sediment bed, the values for θ_{c_g} are those provided by equation (6).

5. Results

5.1. Parameterization for Coefficient *b*

[30] Almost all of the optimized values of b for the 103 individual tests fall in the range [0,1], which is broadly consistent with the results for θ'_{c_i} presented in the literature [*Buffington and Montgomery*, 1997]. However, the distribution of optimized values related to effective stress does not appear to follow any existing critical stress formula. Prompted primarily by the work of *Day* [1980], a dependence on u_* was sought. While there is no apparent consistent relation between b and u_* applicable to all experiments, it is clear (Figure 2) that there does appear to be some functional relationship with bed stress for each set of experiments. Interestingly enough, no further insight is gained by seeking a relation between b and the grain Reynolds number (equation (3)).

[31] The obvious nondimensionalization of shear velocity is using critical shear velocity for the mean, u_{*c_g}. This provides significant improvement in explaining the data scatter (Figure 3), which is not altogether surprising as the use of u_{*c_g} implies information of the mean grain size, confirming that b has a mean grain size dependence.

[32] In addition, a possible shortcoming in u_*/u_{*c_g} as a model for b is the absence of any kind of measure of the magnitude of distribution of sediment sizes in the bed sediments. This absence appears contradictory to the fact that the development of equation (14) arises because of observations of differences between uniform and graded sediments. This suggests that a parameter, which defines the width of the distribution, be included in the functional dependence of b. An obvious parameter of that type is the second central moment of P_i, or σ, the arithmetic standard deviation of particle sizes ("sorting"), given by:

$$\sigma = \sqrt{\sum_{i=1}^{I} (D_i - \overline{D})^2 P_i}, \tag{23}$$

where $\overline{D}$ is an arithmetic mean. As the expression given by equation (14) should reduce to equation (5) in the limit of zero sorting, it seems clear that b should be partially a function of σ [*Parker*, 1990; *Patel and Raju*, 1999; *Shvidchenko et al.*, 2001] and that b should approach zero with σ. This conjecture is supported by previous studies of critical stress which observed that if two surface sediment beds with identical mean grain size are subjected to the same shear stress, under flows with relatively low shear stress, a form such as equation (14) predicts that the distribution with larger σ would result in more entrainment because of nonlinear preferential transport of the finest grains. Indeed, *Wilcock and Crowe* [2003] justify varying the exponent for each size class by observing that, in general, small values of b have been reported for beds when the ratio of sand to gravel is small. *Patel and Raju* [1999] and *Shvidchenko et al.* [2001] found that b was proportional to geometric sorting coefficient $\sigma_{\text{geom}} = \sqrt{D_{84}/D_{16}}$ and also to the absolute value of median grain size for the size fractions smaller than D_g.

[33] It was observed that there was some correlation between the residuals of the relationship shown in Figure 3 and the σ of experimental P_i. In addition, the coefficient of

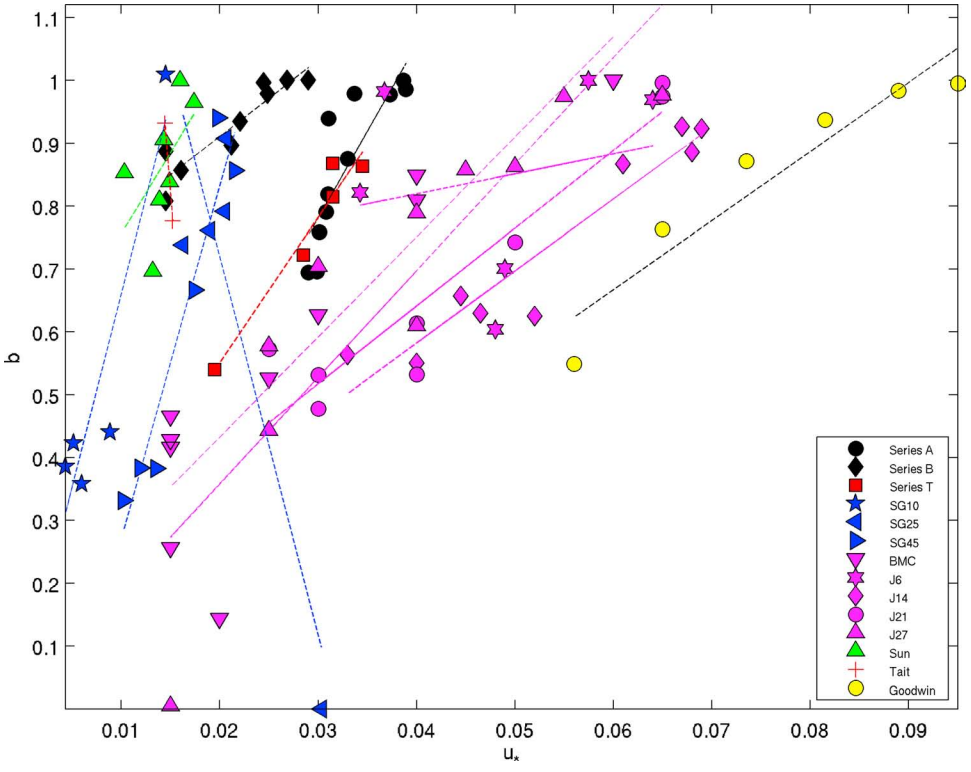

Figure 2. Optimum hiding function exponent b as a function of shear velocity (103 experiments grouped into 14 data sets as shown by the legend. Experimental details in Table 1).

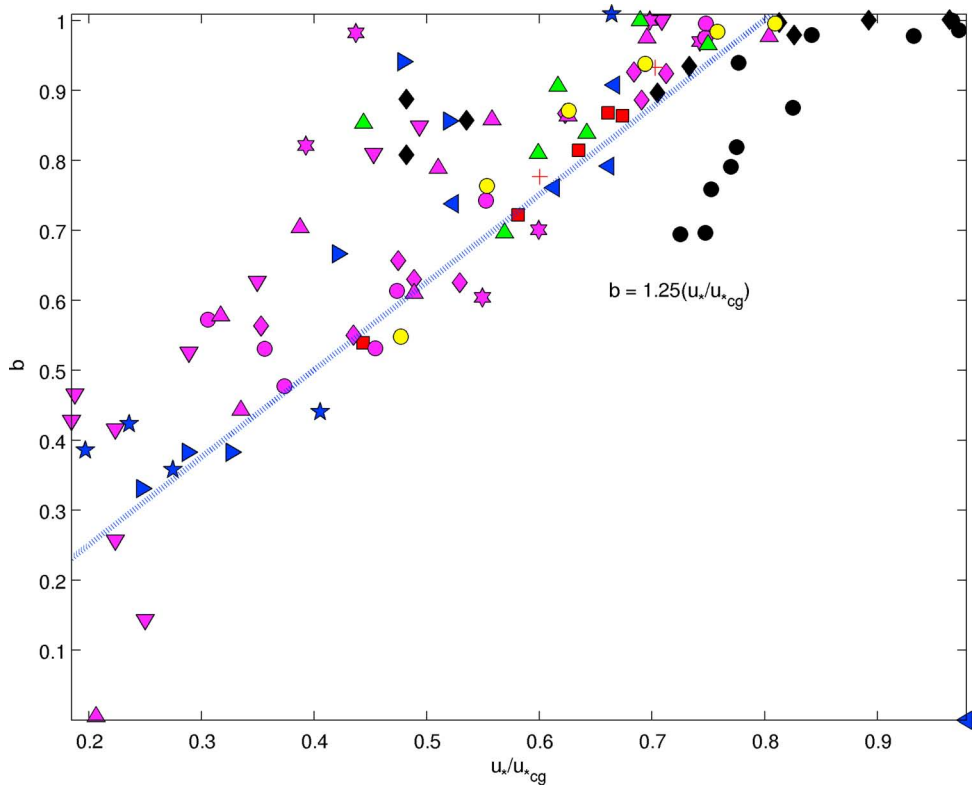

Figure 3. Optimum hiding function exponent b as a function of the ratio of shear velocity and critical shear velocity for D_g. The dotted line is the least squares fit with just zero intercept, along with regression equation. For legend see Figure 2.

variation is slightly smaller than unity for most samples. Motivated by these observations, the product of normalized shear stress and the coefficient of variation (σ/D_g) is a better model for b, as seen in Figure 4. The coefficient-of-variation is arguably a better measure of (particle size) distribution spread because the standard deviation of particle sizes must be understood in the context of the mean of the particle sizes. The coefficient of variation is a scale-invariant dimensionless number, useful for very different mean grain sizes. Further, according to the data presented by *Shvidchenko et al.* [2001], b correlates σ_{geom}/D_g with a coefficient of 0.83. An approximation to the data, in a simple linear form (a single b per flow and bed combination), which give b as a function of D_i, is:

$$b = \gamma\left(\frac{u_*}{u_{*c_g}}\right)\left(\frac{\sigma}{D_g}\right), \tag{24}$$

where a linear least squares fit forced through the origin gives $\gamma = 1.04$. The dashed line in Figure 4 represents this result. Based on a sample size of 103 sets of experiments with different bed sediments and flow conditions, the RMS errors ψ, and scatter index (SI: ratio of mean square error and the mean of observations $\overline{y}$: larger values represent a greater degree of data scatter) associated with equation (24) are shown in Table 2. The residuals between optimized b and that given by equation (24) are uncorrelated. In fact, there were no significant correlations or partial correlations computed between the residuals and any combination of u_*, D_g, and σ which suggests that equation (24) does not include unnecessary parameters.

[34] Further tests were carried out under different assumptions of load dependence using a form of equation (21) modified for the nonstandard assumptions $q^* = \mathbf{f}[(\theta - \theta_e)^{4/2}]$ and $q^* = \mathbf{f}[(\theta - \theta_e)^{5/2}]$. Again, any improvements were inconsistent across experimental data and overall these assumptions did not improve upon the results using equation (21). Using a $q^* = \mathbf{f}[(\theta - \theta_e)^{4/2}]$ model, the slope correction in equation (24) changed from 1.04 to 1.13 and this model for b had an RMS error of 29% (very little change). Using a $q^* = \mathbf{f}[(\theta - \theta_e)^{5/2}]$ model, the slope correction was 0.93, and this model for b had an RMS error of 54%, plus several of the optimized b fell outside of the range 0–1.

5.2. Comparison With Other Parameterizations

[35] In the absence of other explicit models for the behavior of effective stress, the only comparison we can make is with existing predictive relations for b in critical stress models (11) and then apply the assumption that $\theta_e = \theta_c$ ($b = \mathbf{f}(D_g, \sigma)$). Many estimates of the exponent b are created by treating both θ_{c_g} and b as regression coefficients (e.g., *Parker* [1990]; *Kleinhans and van Rijn* [2002]; see also Table 3 by *Bridge and Bennett* [1992]). It is argued that equation (13) loses much of its utility unless the only free parameter is b. In particular, given the relation between D_g and θ_{c_g}, treating θ_{c_g} as a free variable is essentially the same as simply varying D_g. Those parameterizations for b, which avoid these problems and apply in a general fashion, are rare and the authors are aware of only three. The first is

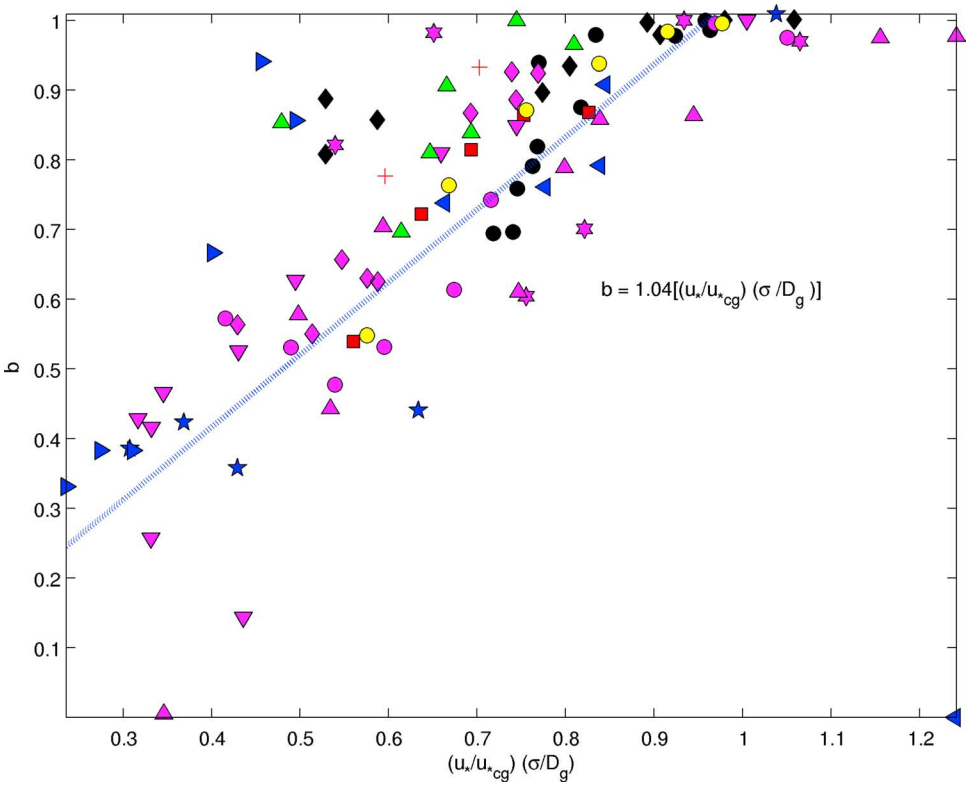

Figure 4. New predictive approximation for hiding function exponent b. The dotted line is the least squares fit with just zero intercept, along with regression equation (24). For legend see Figure 2.

that given by the *Ashida and Michiue* [1972] modification to the *Egiazaroff* [1965] formulation which, using a form consistent with equation (14), can be expressed as,

$$b_i = \begin{cases} \dfrac{1.6667}{\left[\log\left(19\dfrac{D_i}{D_{50}}\right)\right]^2} & \dfrac{D_i}{D_{50}} > 0.6 \\ 0.85\left(\dfrac{D_i}{D_{50}}\right)^{-1} & \dfrac{D_i}{D_{50}} \le 0.6 \end{cases}. \tag{25}$$

[36] The second suggested parameterization for b is that of *Wilcock and Crowe* [2003], given by:

$$b_i = \frac{0.67}{1 + \exp\left(1.5 - \frac{D_i}{D_{\text{geom}}}\right)}, \tag{26}$$

where D_{geom} is a geometric mean. Sorting of the distribution is factored into their approach through the calculation of θ_{c_g} which is a function of the percent of sand on the bed surface, F_s, and given by:

$$\theta_{c_g} = 0.021 + 0.015\exp\left(-20F_s\right). \tag{27}$$

[37] Finally, *Shvidchenko*'s [2001] relation for critical stress is contained in the relations:

Table 2. Model-Observation Mismatch Based on Optimized b

	ψ (%)	SI (-)
Normalized shear stress ($u_*/u_{*_{cg}}$)	51.7	69.73
Equation (24)	28.59	38.57

$$\theta_{c_i} = \begin{cases} \theta_{c_g}\left(\dfrac{D_i}{D_g}\right)^{b-1} & \dfrac{D_i}{D_{50}} \le 1 \\ \theta_{c_g}\left[\log\left(10\dfrac{D_i}{D_g}\right)\right]^{-2.2} & \dfrac{D_i}{D_{50}} \ge 1 \end{cases} \tag{28}$$

$$b = 1 - [2\sigma_{\text{geom}}^{-0.1}(0.049\log\left(1000D_{50}\right)^3 - 0.26\log\left(1000D_{50}\right)^2 + 0.33\log\left(1000D_{50}\right) + 1.2] - 1.4.$$

[38] The relations of *Hayashi et al.* [1980] and *Kleinhans and van Rijn* [2002] have not been included (or examined further) because they are modifications to the practical application, rather than the functional form, of equation (25). While the RMS errors of the new parameterizations are low (Table 2), there is of course no guarantee that numerically optimized b produces better predictions of P_{m_i} within the framework of equation (21), even if the search range for minimization ($[-2, 2]$) is greater than what is physically realistic. Therefore, an additional test of the skill of new parameterization (equation (24)), and the skill of existing models (equations (25), (26), and (28)), were made all within the framework for P_{m_i} given by equation (21).

[39] Skill was assessed using the Jensen-Shannon divergence, a measure of similarity between two proportional distributions given by [*Lin*, 1991]:

$$J(O_{ij}||E_{ij}) = \frac{1}{2}\left[\sum O_{ij}\ln\left(\frac{2O_{ij}}{O_{ij}+E_{ij}}\right) + \sum E_{ij}\ln\left(\frac{2E_{ij}}{O_{ij}+E_{ij}}\right)\right], \tag{29}$$

Table 3. Model Skill: $\sqrt{J}$ Scores for Each Aggregated Experiment Set and Each Model[a]

Experiment	Equation (25)	Equation (28)	Equation (26)	Equation (24)	Percent Difference Between Equations (26) and (24)
Series A	0.4959	0.9914	0.3853	**0.3024**	21.5
Series B	0.6094	0.9757	0.5077	**0.3846**	24.2
Series T	0.3857	0.8511	0.2390	**0.1113**	53.4
SG10	0.3942	0.7225	0.4108	**0.1790**	56.4
SG25	0.2556	0.7658	0.3481	**0.2823**	18.9
SG45	0.3024	0.8653	0.3229	**0.3066**	5.0
BMC	0.5759	0.9140	0.3651	**0.3223**	17.5
J6	0.7336	0.9885	0.5303	**0.3634**	31.5
J14	0.5495	0.9789	0.3544	**0.3128**	11.8
J21	0.5759	0.9140	0.3651	**0.3223**	11.8
J27	0.5582	0.8170	**0.3541**	0.3831	−8.2
Sun	0.5967	0.8301	**0.2327**	0.3021	−29.8
Tait	0.4421	0.9259	0.3288	**0.2457**	25.3
Goodwin	0.7217	0.9481	0.4208	**0.1529**	63.7
Ensemble result	0.3527	0.7983	0.1543	**0.1008**	34.7

[a]The ensemble result has been calculated by combining all data from all experiments. The best scores for each set of experiments and ensemble are in boldface.

where O_{ij} and E_{ij} are the observed and modeled, respectively, of the i-th size class and the j-th test case. As noted by *Endres and Schindelin* [2003], $\sqrt{J}$ is a metric of model performance against observations when both are proportional (distribution) data. Being an information statistic, it does not suffer from sensitivity to sample size like other metrics such as a Brier Skill score. For a nonmathematical review of the properties and application of this and other divergence metrics, see *Cha* [2007]. Smaller values represent better predictions. An example data set (that of *Blom and Kleinhans* [1999]) and typical model comparison are illustrated in Figure 5. The calculated $\sqrt{J}$ for each of the 14 sets of aggregated experiments are summarized in Table 3. The relations proposed here out-perform those proposed by

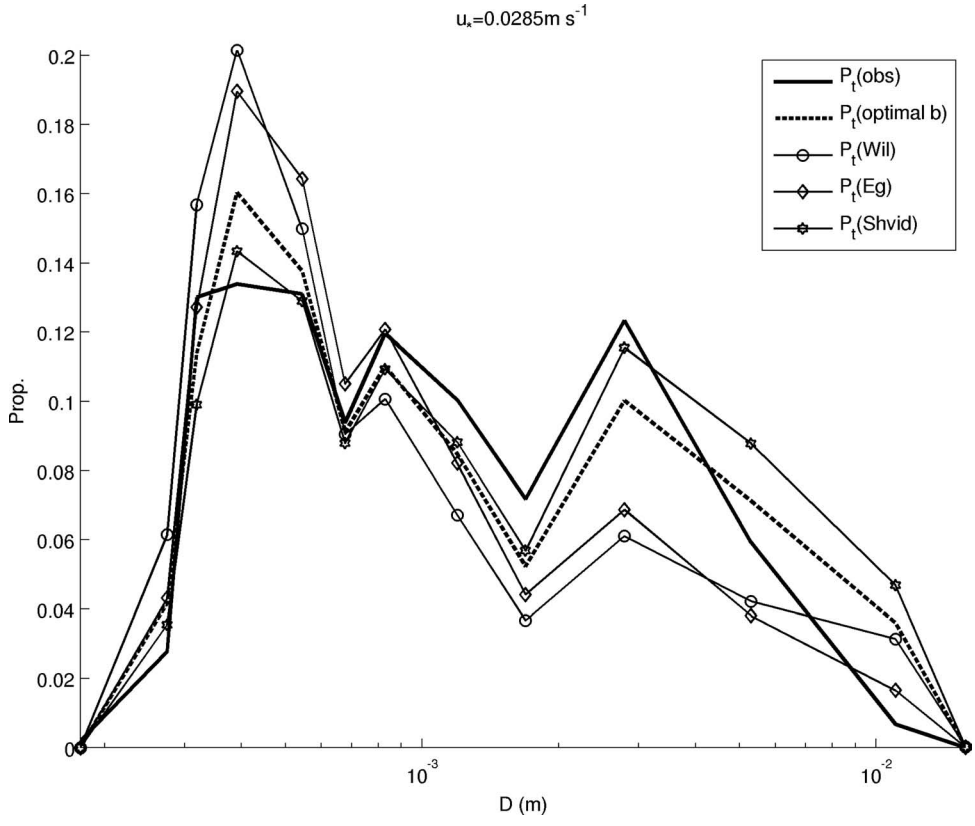

Figure 5. Example model comparison using an experiment from the *Blom and Kleinhans* [1999] data set (corresponding to the shear velocities as shown). Heavy solid line is the measured data. The other lines are the entrainment model with different hiding functions: optimized (heavy dashed line) [*Shvidchenko et al.*, 2001], equation (28), stars, [*Wilcock and Crowe*, 2003], equation (26), circles, [*Egiazaroff*, 1965], equation (25), squares.

Egiazaroff [1965], *Shvidchenko et al.* [2001], and *Wilcock and Crowe* [2003] in 12 of the 14 data sets. In aggregate, the new formula for hiding function given by equation (24) performs the best, with an ensemble $\sqrt{J}$ almost 35% smaller than the best performing prior formula (that of *Wilcock and Crowe* [2003]: 0.10 compared with 0.154).

6. Application

[40] One artifact of adapting functional forms developed for critical stress (equation (11)) in parameterizations of effective stress is that spurious behavior is observed when $D_i > D_g$ and $u_* >> u_{*c_g}$. As a result, the application of equation (24) requires a constraint that for $D_i > D_g$, b is limited to ≤ 1. Therefore, the complete approximation of entrainment threshold for individual size classes in a mixture is suggested as,

$$\theta_{e_i} = \begin{cases} \theta_{c_g}\left(\dfrac{D_i}{D_g}\right)^{\left(1.04\left[\frac{u_*}{u_{*c_g}}\right]\left[\frac{\sigma}{D_g}\right]^{-1}\right)} & \dfrac{D_i}{D_g} \leq 1 \\ \theta_{c_g}\left(\dfrac{D_i}{D_g}\right)^{\min\left[1,\left(1.04\left\{\frac{u_*}{u_{*c_g}}\right\}\left\{\frac{\sigma}{D_g}\right\}^{-1}\right)\right]} & \dfrac{D_i}{D_g} > 1 \end{cases} . \tag{30}$$

[41] Normalized excess stress based on (30) has been plotted as a function of normalized bed stress in Figure 6. Example lines for various relative grain size and coefficients of variation have been presented. In the absence of a mixture of grain sizes, once the threshold condition has been met, excess stress defined using the Shields parameter scaled by u_{*c_g} will be a linear function of bed stress scaled by u_{*c_g} and will, by definition, be invariant to changes in grain size (through the dependence of u_{*c_g} on D; Figure 6, dotted lines in all plots). Examining equation (30) for cases of mixed grain sizes, however, shows that excess stress will increase nonlinearly with scaled bed stress except for the condition $D_i = D_g$, where equation (30) reduces to the critical Shields parameter. At low τ, σ has a greater effect on excess stress. For a grain diameter less than the mean, the effective stress is increased relative to critical stress, but the amount of this increase is progressively lowered with increasing sorting. The τ at which, for each $D_i/D_g < 1$, τ_e becomes less than τ_c is inversely related to σ (in other words, small σ raises the τ at which the condition $\tau_e < \tau_c$ applies). For $D_i > D_g$, τ_e is always less than τ_c, and σ has less effect at low τ.

[42] The application of this formula to predict the rate and size of sediment in transport for a given set of flow and sediment conditions requires knowledge of D_i, P_I, and shear velocity. Equation (30) defines the computation of effective stress, where θ_{c_g} is calculated according to equation (6) for the mean particle size, and particle size arithmetic standard deviation according to equation (23). We have not specified a particular surface transport model and the

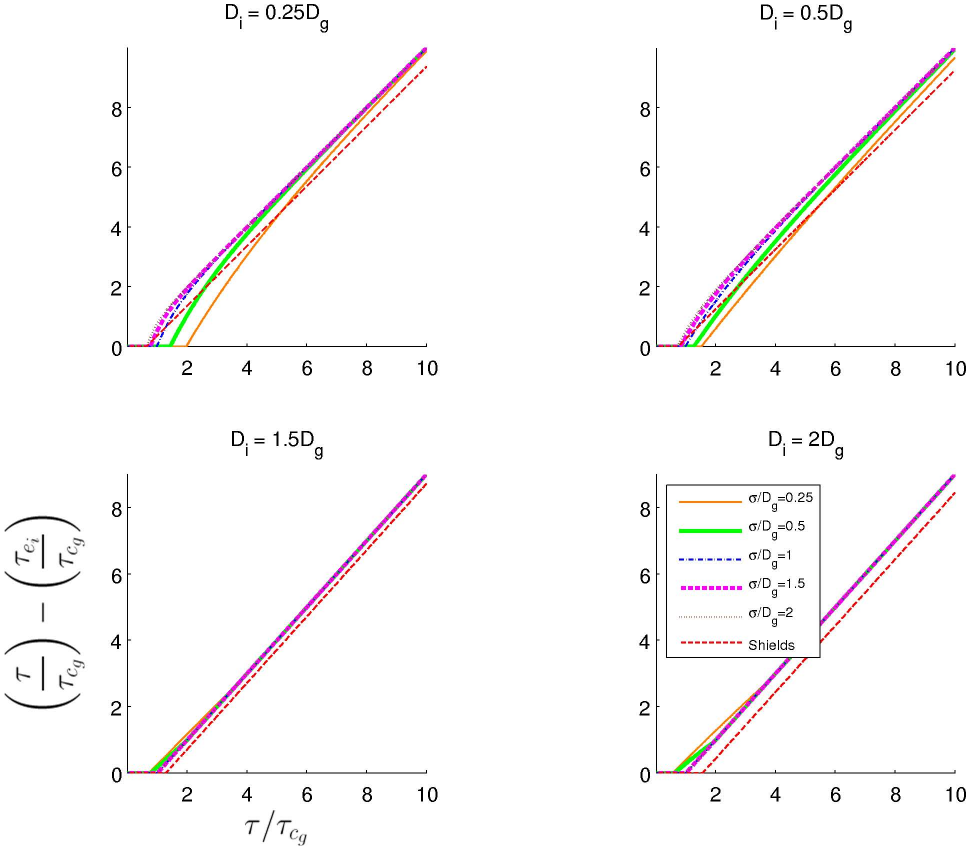

Figure 6. Plots of scaled stress versus scaled excess stress, as predicted by equation (30), for different grain sizes (each panel) and different coefficients of variation (σ/D_g; each line). For reference, the excess stress as predicted for that grain size using the Shields criterion is the dashed line.

excess stress determined from applying the effective stress as specified in (30) can be utilized in any transport formulation where $q^* = \mathbf{f}[(\theta - \theta_e)^{3/2}]$ [e.g., *Meyer-Peter and Müller*, 1948; *Einstein*, 1950; *Bagnold*, 1956; *Fernandez-Luque and Van Beek*, 1976]. As mentioned above, the coefficients in equation (30) can be optimized for other commonly adopted transport models such as $q^* = \mathbf{f}[(\theta - \theta_e)^{4/2}]$ and $q^* = \mathbf{f}[(\theta - \theta_e)^{5/2}]$.

[43] The development of equation (24) primarily used data from flumes that recirculate both sediment and water (Table 1). Though not by design, this has aided the formulation of equation (24) because in such cases transport is flow-regulated because bed sediment grain size remains nearly constant [*Parker and Wilcock*, 1993; *Rubin and Topping*, 2001]. In natural situations, changes in bed sediment composition (caused by winnowing or episodic sediment supply) will affect P_i and possibly D, therefore D_g and σ. In this respect, practical application of our approach to excess stress (equation (30)) is no different from previous formulations based on equation (11) in that it is sensitively dependent on estimates of the bed sediment particle size distribution. *Chen and Stone* [2008] refer to this as an "intrinsic uncertainty" of mixed sediment transport rate estimates due to the composition of the bed sediment. Predictions of bed particle-size distribution are very sensitive to fractional sediment transport predictions as well as an incomplete knowledge of sediment supply. Sampling surface grain-size distribution (specification of P_i) is difficult under energetic conditions, although recently developed technologies for collecting in situ images of bed sediment [*Rubin et al.*, 2007; *Blanpain et al.*, 2009] in conjunction with automated algorithms for grain size estimates [*Rubin*, 2004; *Buscombe et al.*, 2010] should help such efforts.

[44] As with any excess stress formulation, changes to bed morphology and channel slope could affect field implementation, although this is not important in the flume data upon which the fractional effective stress given by (30) is based. In which case, the effects on flow such as secondary currents, drag, wakes, and flow separation would have to be represented through calculated u_*.

7. Discussion

[45] The chosen framework for this study (equation (13)) incorporates the often-used hypothesis that a single fractional transport function can be defined in terms of the excess stress $(\theta - \theta_e)$ using similarity principles [*Ashida and Michiue*, 1972; *Wilcock*, 1988]. Defining effective stress in terms of a correction to the Shields stress for the mean particle diameter (equation (13)) using an exponent b, we have used inverse methods to find that $b = \mathbf{f}[\theta]$, which challenges the commonly adopted assumption that $\theta_e = \theta_{c_i}$, and suggests that excess stress, as a representation of the component of bed shear stress that is available for transporting sediment, is misrepresented by the notion of a critical stress for each particle size based on the mean and standard deviation of particle sizes present. A dependence of θ_e on u_* reflects the change in magnitude of effective stress as the flow itself changes. This result is consistent with the findings of previous researchers [e.g., *Day*, 1980; *Ashworth and Ferguson*, 1989] who have reported differing optimal b for constant values D_i/D_g with differing flow conditions.

[46] We observe that b is foremost dependent on normalized shear stress, and second, on the ratio of sorting to mean grain size (Table 2), and conclude that our parameterization of b improves upon the next best alternative (the substitution of critical stress as defined by *Wilcock and Crowe* [2003] for effective stress) in 12 out of 14 data sets and on aggregate (evaluated against 103 individual experimental sediment and flow combinations), presumably because it contains information on the flow. Much of the scatter in the proposed formula for b is probably due to differences between the size distribution of the bulk material and the surface, which is interacting with the flow. Here both surface-based and bulk-based bed-size distributions are mixed, which perhaps constitutes the greatest uncertainty in the data sets used in this study.

[47] The new relation for effective shear stress is based on a commonly used dependence of fractional transport rate q_i on $(\theta - \theta_e)^{3/2}$, and on a predictive relationship identified for b which has been evaluated on its ability to reproduce the mobilized grain-size distribution, P_{m_i}, from the measured integrated transport load across the whole range of D_i. This avoids many uncertainties in previous approaches which compare modeled and measured fractional transport rates, and requires adopting a fraction-specific reference stress as well as a specific transport model.

[48] The new formulation for b (equation (24)) goes to zero (the condition of no mitigation of selective fine mobilization) with σ and u_*. Therefore, when σ goes to zero (no distribution of grain sizes) θ_e becomes Shields stress (θ_{c_g}).

[49] The necessity of a hiding function is widely conjectured to be due to the combined effects of greater exposure of the coarse grains to the flow, and finer grains partially hidden by the coarser particles. With reference to Figure 6, for grain sizes finer than the mean ($D_i < D_g$), the effects of the mixture are to make the grain harder to entrain than predicted by critical Shields (equation (6)) at low τ, but easier to entrain at high τ. In contrast, at any τ it is easier to entrain grains larger than the mean ($D_i > D_g$) compared to the critical Shields parameter. Predicted excess stresses are relatively insensitive to sorting (σ) at higher τ. At low τ, sorting affects the excess stress much more for smaller grains compared to larger grains. In general (i.e., for all τ), increasing σ makes it harder to entrain a grain smaller than the mean (greater stresses are required for the same excess stress). In contrast, increasing σ makes it easier to entrain a grain larger than the mean, but only until some τ beyond which σ has no effect.

[50] In energetic flows, studies have shown that there is no distinction between mobilized and source-size distributions [*Nielsen*, 1983; *Hay and Sheng*, 1992; *Wang et al.*, 1998], even up to 1 m water depth in very energetic flows [*Battisto*, 2000], which might explain vertical profiles of uniform grain size at high shear stresses [e.g., *Bennett et al.*, 1998]. Using a classic approach for mobilizing mixtures such as equation (12), such a situation would be explained if, in the absence of supply limitation for all i, $\theta >> \theta'_{c_i}$. The competing hypothesis put forward here is that under these very high bed stresses there is an absence of preferential transport, therefore observed situations of negligible difference between bed and mobilized grain size arise because the mobilization criterion changes with flow conditions.

[51] While the observations used in this study indicate selective mobilization of the sediment bed at low excess stress, repeated observations at high excess stress indicate mobilized distributions which mirror the source distribution [*Nielsen*, 1983; *Hay and Sheng*, 1992; *Wang et al.*, 1998], even up to 1 m water depth in very energetic flows [*Battisto*, 2000]. This might explain vertical profiles of uniform grain size at high shear stresses [e.g., *Bennett et al.*, 1998]. This behavior cannot be explained by any of the classical excess stress formulations based on critical stress and, in fact, requires precisely the type of behavior exhibited in Figure 6 and predicted by an effective stress determined through the application of equation (30).

8. Conclusions

[52] The concept of effective stress (θ_e), defined as the amount of stress (θ) which does not contribute to mobilizing sediment, is applied to graded sediment (a mixture of grain sizes) using an approach commonly employed for fractional critical stress (θ_c) for graded sediment. We adopt a commonly used dependence of fractional transport rate on $(\theta - \theta_e)^{3/2}$, which was evaluated using the mobilized particle-size distribution (P_{m_i}) rather than transport rates, because this approach avoids the necessity to select a specific transport formulation and requires measurements only of the transported sediment distribution.

[53] Effective stress is found to be a function of bed sediment sorting and grain size, and a function of flow conditions (θ), which challenges the commonly held assumption that it is always equal to the critical stress. This suggests that excess stress, as a representation of the component of bed shear stress that is available for transporting sediment, is misrepresented by the notion of a critical stress for each particle size based on the mean and standard deviation of the particle sizes present.

[54] A new parameterization for fractional effective stress was developed following a classical approach to the problem of mitigating the bias toward fine material in mobilization relations. This method employs a so-called "hiding" exponent to quantify the distribution effects on fraction-specific mobilization, but the developed parameterization reduces to the classic Shields-type critical stress for the uniform grain size case. The proposed function outperforms the next best existing formula in 12 of the 14 data sets tested (103 individual bed sediment distributions and flow conditions), and on aggregate by 34%. The identified relation exhibits behavior which is consistent with seemingly contradictory observations of selective mobilization at low excess stress and uniform mobilization at high excess stress.

[55] **Acknowledgments.** The work was funded by a (UK) Natural Environment Research Council grant (NE/G007543/1) awarded to D.C. The authors thank Peter Wilcock, Sean Bennett, and an anonymous reviewer for their constructive comments which collectively made for significant improvements to the manuscript.

References

Ackers, P., and W. White (1973), Sediment transport: New approach and analysis, *Proc. Am. Soc. Civ. Eng.*, *99*, 2041–2060.

Allen, J. (1985), *Principles of Physical Sedimentology*, 272 pp., Allen and Unwin, London, UK.

Ashida, K., and M. Michiue (1972), Study on hydraulic resistance and bedload transport rate in alluvial streams, *Trans. Japan Soc. Civ. Eng.*, *206*, 59–69.

Ashworth, P., and R. Ferguson (1989), Size-selective entrainment of bed load in gravel bed streams, *Water Resour. Res.*, *25*, 627–634.

Bagnold, R. (1956), The flow of cohesionless grains in fluids, *Philos. Trans. R. Soc., A*, *249*, 235–297.

Bagnold, R. (1973), The nature of saltation and of "bed-load" transport in water, *Proc. R. Soc. London, Ser. A*, *332*, 473–504.

Battisto, G. M. (2000), Field measurements of mixed grain size suspension in the nearshore under waves, M.S. thesis, College of William and Mary, Va.

Bennett, S., J. Bridge, and J. Best (1998), Fluid and sediment dynamics of upper stage plane beds, *J. Geophys. Res.*, *103*, 1239–1274.

Blanpain, O., P. B. du Bois, P. Cugier, R. Lafite, M. Lunven, J. Dupont, E. Le Gall, J. Legrand, and P. Pichavant (2009), Dynamic sediment profile imaging system (DySPI): A new field method for the study of dynamic processes at the sediment-water interface, *Limnol. Oceanogr. Methods*, *7*, 8–20.

Blom, A., and M. Kleinhans (1999), Non-uniform sediment in morphological equilibrium situations, *Tech. Tep., Sand Flume Exps. 97/98*, Univ. of Twente, Rijkswaterstaat RIZA, WL/Delft Hydraulics, Netherlands.

Bridge, J., and S. Bennett (1992), A model for the entrainment and transport of sediment grains of mixed sizes, shapes and densities, *Water Resour. Res.*, *28*, 337–363.

Buffington, J., and D. Montgomery (1997), A systematic analysis of eight decades of incipient motion studies, with special reference to gravel-bedded rivers, *Water Resour. Res.*, *33*(8), 1993–2029.

Buffington, J., W. E. Dietrich, and J. W. Kirchner (1992), Friction angle measurements on a naturally formed gravel streambed: Implications for critical boundary shear stress, *Water Resour. Res.*, *28*, 411–425.

Buscombe, D., D. M. Rubin, and J. W. Warrick (2010), A universal approximation to grain size from images of non-cohesive sediment, *J. Geophys. Res.*, *115*, F02015, doi:10.1029/2009JF001477.

Carling, P. A. (1983), Threshold of coarse sediment in broad and narrow natural streams, *Earth Surf. Processes Landforms*, *8*, 1–18.

Cha, S. (2007), Comprehensive survey on distance/similarity measures between probability density functions, *Int. J. Math. Models Methods Appl. Sci.*, *1*, 300–307.

Chen, L., and M. C. Stone (2008), Influence of bed material size heterogeneity on bedload transport uncertainty, *Water Resour. Res.*, *44*, W01405, doi:10.1029/2006WR005483.

Cheng, N. (2004), Analysis of bedload transport in laminar flows, *Adv. Water Resour.*, *27*, 937–942.

Cheng, N. (2006), Influence of shear stress fluctuation on bed particle instability, *Phys. Fluids*, *18*, 096602.

Day, T. (1980), A study of the transport of graded sediments, *Tech. Rep. IT 190*, Hydraulics Research Station, Wallingford, UK.

Diplas, P., and J. Frip (1992), Properties of various sediment sampling procedures, *J. Hydraul. Eng.*, *118*, 955–970.

Egiazaroff, I. (1965), Calculation of non-uniform sediment concentration, *J. Hydraul. Eng.*, *91*, 225–247.

Einstein, H. (1950), The bed-load function for sediment transportation in open channel flows, *Tech. Rep. 1026*, 71 pp., USDA Soil Conservation Service, Washington, D.C.

Endres, D. M., and J. E. Schindelin (2003), A new metric for probability distributions. *IEEE Trans. Inf. Theory*, *49*, 1858–1860.

Fernandez-Luque, R., and R. Van Beek (1976), Erosion and transport of bed-load sediment, *J. Hydraul. Res.*, *14*, 127–144.

Hammond, F., A. Heathershaw, and D. Langhorne (1984), A comparison between Shields' threshold criterion and the movement of loosely packed gravel in a tidal channel, *Sedimentology*, *31*, 51–62.

Hanes, D., and A. Bowen (1985), A granular fluid model for steady intense bed-load, *J. Geophys. Res.*, *C5*, 9149–9158.

Hay, A. E., and J. Sheng (1992), Vertical profiles of suspended sand concentration and size from multifrequency acoustic backscatter, *J. Geophys. Res.*, *97*, 15,661–15,677.

Hayashi, T., S. Ozaki, and T. Ichibashi (1980), Study on bed load transport of sediment mixture, in *Proceedings, 24th Japanese Conference on Hydraulics*, pp. 35–43.

Kachel, N., and R. Sternberg (1971), Transport of bedload as ripples during an ebb current, *Mar. Geol.*, *10*, 229–244.

Kellerhals, R., and D. Bray (1971), Sampling procedures for coarse fluvial sediments, *J. Hydraul. Eng.*, *97*, 1165–1180.

Kleinhans, M., and L. van Rijn (2002), Stochastic prediction of sediment transport in sand-gravel bed rivers, *J. Hydraul. Eng.*, *128*(4), 412–425.

Komar, P. D. (1987), Selective grain entrainment by a current from a bed of mixed sizes: A reanalysis, *J. Sediment. Petrol.*, *57*(2), 203–211.

Kuhnle, R. A. (1992), Fractional transport rates of bedload on Goodwin Creek, in *Dynamics of Gravel Bed Rivers*, edited by P. Billi et al., pp. 142–155, John Wiley, N. Y.

Kuhnle, R. A. (1993), Incipient motion of sand-gravel mixtures, *J. Hydraul. Eng.*, *119*, 1400–1415.

Lajeunesse, E., L. Malverti, and F. Charru (2010), Bed load transport in turbulent flow at the grain scale: Experiments and modeling, *J. Geophys. Res.*, *115*, F04001, doi:10.1029/2009JF001628.

Lin, J. (1991), Divergence measures based on the Shannon entropy, *IEEE Trans. Inf. Theory*, *37*, 145–151.

Madsen, O., and W. Grant (1976), Sediment transport in the coastal environment, *Tech. rep. 209, Ralph M. Parson Lab. for Water Research and Hydrodynamics*, Dept.ment of Civil Engineering, MIT, Mass., 105 pp.

Meyer-Peter, E., and R. Müller (1948), Formulas for bed-load transport, *Report on 2nd Meeting of International Association for Hydraulic Research*, pp. 39–64, Int. Assoc. for Hydraulic Struct. Res., Stockholm, Sweden.

Milhous, R. (1973), Sediment transport in a gravel-bottomed stream, Ph.D. thesis, Oregon State University, Corvallis.

Nielsen, P. (1983), Entrainment and distribution of different sand sizes under water waves, *J. Sediment. Petrol.*, *53*, 423–428.

Nielsen, P. (1992), *Coastal Bottom Boundary Layers and Sediment Transport*, 324 pp., World Scientific, Singapore.

Parker, G. (1990), Surface-based bedload transport relation for gravel rivers, *J. Hydraul. Res.*, *28*, 417–436.

Parker, G., and P. Klingeman (1982), On why gravel bed streams are paved, *Water Resour. Res.*, *18*(5), 1409–1423.

Parker, G., and P. R. Wilcock (1993), Sediment feed and recirculating flumes—fundamental difference, *J. Hydraul. Eng.*, *119*(11), 1193–1204.

Parker, G., P. Klingeman, and D. McLean (1982), Bedload and size distribution in paved gravel-bed streams, *J. Hydraul. Am. Soc. Civ. Eng.*, *108*, 544–571.

Patel, P., and K. Raju (1999), Critical tractive stress of nonuniform sediments, *J. Hydraul. Eng.*, *37*(1), 39–58.

Pender, G., and Q. Li (1995), Comparison of two hiding function formulations for non-uniform sediment transport calculations, in *Proceedings of the Institute of Civil Engineers, Water, Maritime, and Energy, 112*, pp. 127–135, Inst. of Civil Eng., London, doi:10.1680/iwtme.1995.27658

Proffitt, G. T., and A. J. Sutherland (1983), Transport of non-uniform sediments, *J. Hydraul. Res.*, *21*(1), 33–43.

Rubin, D. (2004), A simple autocorrelation algorithm for determining grain size from digital images of sediment, *J. Sediment. Res.*, *74*, 160–165.

Rubin, D. M., and D. Topping (2001), Quantifying the relative importance of flow regulation and grain-size regulation of suspended-sediment transport (α) and tracking changes in grain size on the bed (β), *Water Resour. Res.*, *37*, 133–146.

Rubin, D. M., H. Chezar, J. N. Harney, D. J. Topping, T. S. Melis, and C. R. Sherwood (2007), Underwater microscope for measuring spatial and temporal changes in bed-sediment grain size, *Sediment. Geol.*, *202*, 402–408.

Sambrook-Smith, G., A. Nicholas, and R. Ferguson (1997), Measuring and defining bimodal sediments: Problems and implications, *Water Resour. Res.*, *33*, 1179–1185.

Sawamoto, M., and T. Yamashita (1986), Sediment transport due to wave action, *J. Hydrosci. Hydraul. Eng.*, *4*, 1–15.

Shields, A. (1936), Application of similarity principles and turbulence research to bedload movement, *Tech. Rep. 167, Hydrodynamics Laboratory*, California Institute of Technology, Pasadena, Calif.

Shvidchenko, A., G. Pender, and T. Hoey (2001), Critical shear stress for incipient motion of sand/gravel streambeds, *Water Resour. Res.*, *37*(8), 2273–2283.

Sleath, J. (1978), Measurements of bed load in oscillatory flow, *J. Waterw. Port Coastal Ocean Eng.*, *104*, 291–307.

Soulsby, R. (1997), *Dynamics of Marine Sands: A Manual for Practical Applications*, 249 pp., Thomas Telford, London, UK.

Sumer, B., L. Chua, N. Cheng, and J. Fredsoe (2003), Influence of turbulence on bed load sediment transport, *J. Hydraul. Eng.*, *129*, 585–596.

Sun, Z., and J. Donahue (2000), Statistically derived bedload formula for any fraction of nonuniform sediment, *J. Hydraul. Eng.*, *126*(2), 105–111.

Tait, S., B. Wiletts, and J. Maizels (1992), Laboratory observations of bed armouring and changes in bedload composition, in *Dynamics of Gravel-Bed Rivers*, edited by P. Billi et al., pp. 205–225, John Wiley, N. Y.

van Rijn, L. C. (2007), Unified view of sediment transport by currents and waves. III: Graded beds, *J. Hydraul. Eng.*, *133*(7), 761–775.

Wang, P., R. A. Davis, and N. C. Kraus (1998), Cross-shore distribution of sediment texture under breaking waves along low-wave-energy coasts *J. Sediment. Petrol.*, *68*, 497–506.

Wiberg, P., and J. Smith (1987), Calculations of the critical shear stress for motion of uniform and heterogeneous sediment, *Water Resour. Res.*, *23*, 1471–1480.

Wiberg, P., and J. Smith (1989), Model for calculating bed load transport of sediment, *J. Hydraul. Eng.*, *115*, 101–123.

Wilcock, P. R. (1988), Methods for estimating the critical shear stress of individual fractions in mixed-size sediment, *Water Resour. Res.*, *24*(7), 1127–1135.

Wilcock, P., and J. Crowe (2003), Surface-based transport model for mixed-size sediment, *J. Hydraul. Eng.*, *129*(2), 120–128.

Wilcock, P. R., and B. W. McArdell (1993), Surface-based fractional transport rates: Mobilization thresholds and partial transport of a sand-gravel sediment, *Water Resour. Res.*, *29*(4), 1297–1312.

Wilcock, P. R., and J. B. Southard (1988), Experimental-study of incipient motion in mixed-size sediment, *Water Resour. Res.*, *24*(7), 1137–1151.

Wilcock, P., S. Kenworthy, and J. Crowe (2001), Experimental study of the transport of mixed sand and gravel, *Water Resour. Res.*, *37*(12), 3349–3358.

Wong, M., and G. Parker (2006), Reanalysis and correction of bed-load relation of Meyer-Peter and Müller using their own database, *J. Hydraul. Eng.*, *132*, 1159.

Wu, W., S. Yang, and Y. Jia (2000), Nonuniform sediment transport in alluvial rivers, *J. Hydraul. Res.*, *38*, 427–434.

Yang, C., and S. Wan (1991), Comparisons of selected bed-material load formulas, *J. Hydraul. Eng.*, *117*, 973–989.

Zanke, U. (2003), On the influence of turbulence on the initiation of sediment motion, *Int. J. Sediment Res.*, *18*, 17–31.

D. Buscombe and D. C. Conley, School of Marine Science and Engineering, University of Plymouth, Drake Circus, Plymouth PL4 8AA, UK. (daniel.buscombe@plymouth.ac.uk)